AEOSR-TR- 91 0808

Grant No. AFOSR-88-0119

A NEW TECHNIQUE FOR TEMPERATURE AND SPECIE CONCENTRATION MEASUREMENTS IN UNSEEDED SUPERSONIC AND HYPERSONIC GAS FLOWS

Principal Investigators:
Daniel A. Erwin
Joseph A. Kunc
E. Phillip Muntz

Department of Aerospace Engineering
University of Southern California
University Park
Los Angeles, California 90089-1191

August 09, 1991

Final Technical Report
Period: February 02, 1988 to February 01, 1991

Air Force Office of Scientific Research
Bolling Air Force Base
Washington, D.C. 20332-6448

UNCLASSIFIED

REPORT DOCUMENTATION PAGE

Form Approved
OMB No. 0704-0188

1. AGENCY USE ONLY (Leave blank)	2. REPORT DATE	3. REPORT TYPE AND DATES COVERED
	9 AUG 91	Final, 2 FEB 88 - 1 Feb 91

4. TITLE AND SUBTITLE
A New Technique For Temperature and Specie Concentration Measurements In Unseeded Supersonic & Hypersonic Gas Flows

5. FUNDING NUMBERS
AFOSR-
88-0119

6. AUTHOR(S)
Daniel Erwin, Joseph Kunc, E. Philip Muntz

7. PERFORMING ORGANIZATION NAME(S) AND ADDRESS(ES)
University of Southern California
Dept of Aerospace Engineering
University Park
Los Angeles, CA 90089-1191

8. PERFORMING ORGANIZATION REPORT NUMBER

9. SPONSORING/MONITORING AGENCY NAME(S) AND ADDRESS(ES)
AIR FORCE OFFICE OF SCIENTIFIC RESEARCH
DIRECTORATE OF AEROSPACE SCIENCES
BOLLING AFB, DC 20332-6448

10. SPONSORING/MONITORING AGENCY REPORT NUMBER
2307/A1

11. SUPPLEMENTARY NOTES

12a. DISTRIBUTION/AVAILABILITY STATEMENT
APPROVED FOR PUBLIC RELEASE
DISTRIBUTION IS UNLIMITED

12b. DISTRIBUTION CODE

13. ABSTRACT *(Maximum 200 words)*

The goal was to develop an experimental diagnostic technique suitable for gas flows of densities intermediate between atmospheric and rarefied. A laser assisted Electron Beam Fluorescense technique which we call electron-photon fluorescense was developed. Theoretical work was done to predict the time dependence of the excitation/deexcitation processes.

14. SUBJECT TERMS
Electron Beam Fluorescense, Hypersonic Flow, Rarefied Gas

15. NUMBER OF PAGES
13

16. PRICE CODE

17. SECURITY CLASSIFICATION OF REPORT	18. SECURITY CLASSIFICATION OF THIS PAGE	19. SECURITY CLASSIFICATION OF ABSTRACT	20. LIMITATION OF ABSTRACT
UNCLASSIFIED	UNCLASSIFIED	UNCLASSIFIED	

Contents

1 Introduction

As described in the original proposal, our goal in this work was the attainment of an experimental diagnostic technique suitable for gas flows of densities intermediate between atmospheric ($N \gtrsim 10^{19}$ cm^{-3}) and rarefied ($N \lesssim 10^{17}$ cm^{-3}). Measurements in such 'intermediate-density' flows, typical of hypersonic flight at altitudes above about 50 km, present difficulties in that traditional wind-tunnel techniques (shadow and schlieren, as well as laser-based scattering techniques) provide insufficient signal. Moreover, the resonant scattering techniques may require an absorptive species as a tracer to be seeded into the flow, a requirement inconsistent with the realities of existing large facilities. On the other hand, the densities are not low enough for continuous electron beam fluorescence (EBF) to be used due to beam spreading and collisional quenching (described below).

EBF has been accepted for many years as the best available tool for investigating rarefied flows.[1,2] In EBF, a continuous beam of energetic ($E \sim$ 15–40 keV) electrons passes through the flow, exciting the molecules, which emit fluorescence whose intensity and spectral properties provide information concerning the density and energy distribution, respectively, of molecules in the flow. The fluorescence may be imaged from a small region along the beam, providing effectively a point measurement, or from the length of the beam, providing a one-dimensional visualization along the line of the beam. The beam may be scanned across the flow using a magnetic field, providing two-dimensional visualization; this has been used in at least one case to investigate low-density supersonic mixing.

At densities higher than about 10^{17} cm^{-3}, the beam begins to suffer significant spreading due to interaction with the gas. Moreover, molecules excited by the beam are collisionally deexcited without radiation at a rate proportional to the gas density; when this rate becomes large compared to the fluorescence rate, the EBF signal loses its dependence on density.

EBF in rarefied flows is not a time-resolved technique. In such flows, however, turbulence is not generally an issue, so this is not a problem. On the other hand, the intermediate-density hypersonic regime presents a requirement for submicrosecond time resolution.

We proposed to overcome the above limitations using a laser-assisted EBF technique which we called electron-photon fluorescence or EPF. This involved using pulsed laser-induced fluorescence to probe the excited ions generated by an electron beam. The signal generated by such a probe is time-resolved to 50 ns or less. In the regime where the ordinary EBF signal is quenched, the time average of the EPF signal is also quenched, but the peak is fully density-dependent. This is discussed in detail in ref. [3].

After the work began, we became aware of a technique[4] for generating intense ($I \gtrsim 100$ A) pulsed electron beams using a triggered pseudospark discharge. Using the pulsed beam, the peak of the time-dependent pulsed EBF signal (PEBF) is again quench-free just as is that of EPF. However, the apparatus is much simpler, requiring no laser. Moreover, the amount of light generated by the high-current pulsed beam could be expected to be very large, allowing single-pulse visualization of (for example) mixing dynamics.

In the following sections, the experimental work is described in detail. In addition, we describe our theoretical work to predict the time dependence of the excitation/deexcitation processes.

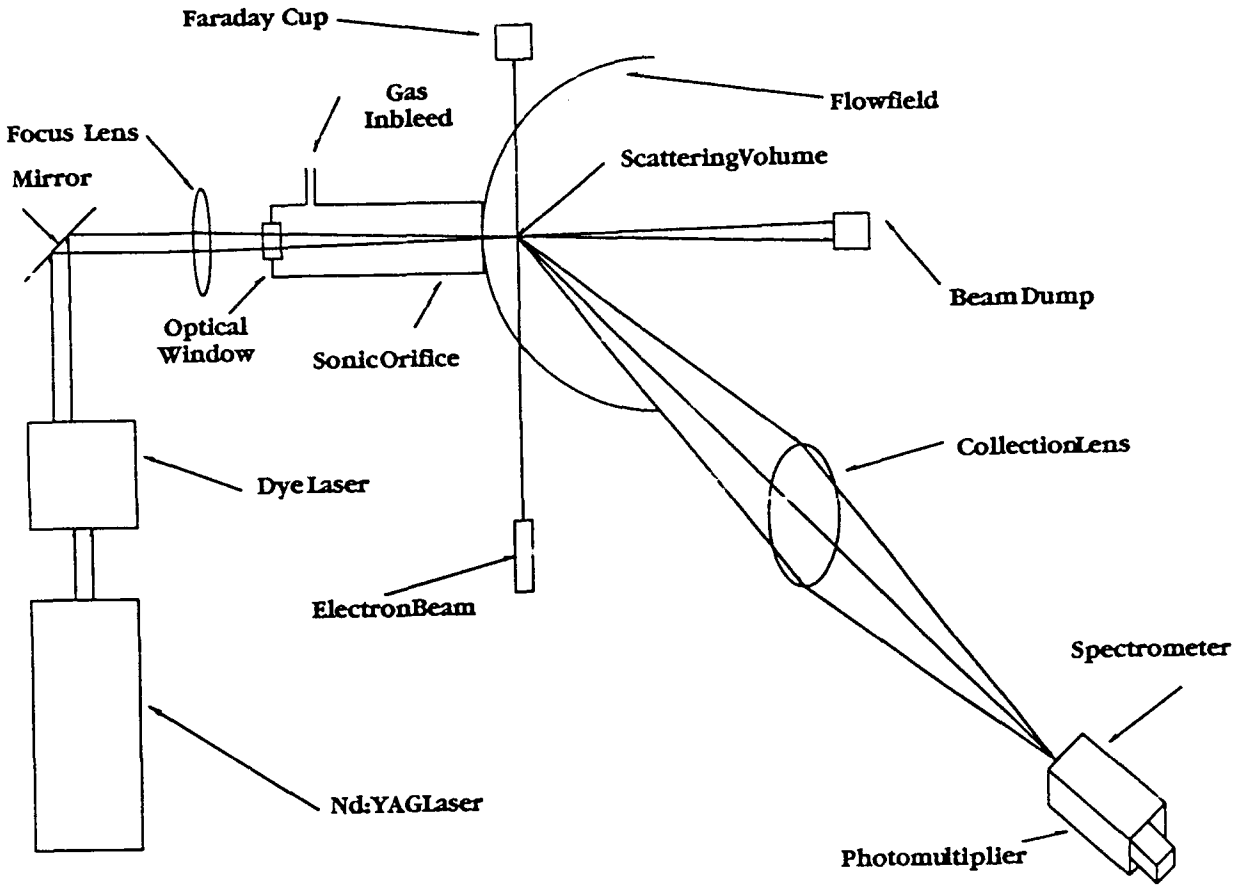

Figure 1: Setup of the electron-photon fluorescence experiment.

2 Experimental Work

2.1 Electron-Photon Fluorescence

As one of the alternative modes for EPF, C-W operation is of interest to investigate. We had available appropriate electron beam equipment (Brad Thomson electron beam welder) that could easily produce a 20 to 30 ma, 1–2 mm diameter beam in a high-density nitrogen flow. The nitrogen flow was created in the USC low density wind tunnel using a free-jet expansion through a 5-mm-diameter orifice. The low density wind tunnel is a cryogenically pumped facility that is capable of maintaining 3×10^{-4} torr with a mean flow of 0.3 gm/sec. Thus, at positions within a few orifice diameters of the orifice, the nitrogen number density could be maintained at around 10^{18} cm^{-3}. The low corresponding pumping pressure in the facility allowed easy injection of the electron beam into the high-density flow.

The experimental setup is illustrated in fig. 1. the laser beam was introduced through the plenum exiting the sonic orifice along the gas flow axis. This beam was focused using a 1000-cm-focal-length lens to a point approximately two exit diameters downstream along the flow axis. The electron beam was injected perpendicular to the flow axis and passed through the laser beam focal volume, creating a mutual scattering volume. Light produced from the interaction of the laser and electron beam with the flowing nitrogen molecules within this scattering volume was collected at 90° to the scattering plane formed by the crossed electron and laser beams by a system of lenses. This light was then focused onto the entrance slit of a 0.5-m Spex Industries Model 1870 spectrometer. The radiation was detected using a RCA

C31034A photomultiplier tube, whose signal was processed using a Stanford Research gated integrator system. A Stanford Research pulse generator was used to control both the laser firing sequence and detector system.

In order to create an induced fluorescence signal in the (0,0) band of the first negative system of N_2^+ whose bandhead is at 3914.4 Å, it is necessary to produce a pump beam at this wavelength. The Nd:YAG laser which was available for use in this experiment is a Quanta-Ray DCR-1, supplied by the Air Force Phillips Laboratory, Rocket Propulsion Directorate. In order to produce the necessary pump wavelength with this laser, a frequency-tripling crystal was required to convert the primary 1.06 μm beam to 355 Å. This beam was then used to pump a dye laser (Quanta-Ray PDL-1, also supplied by the Phillips Laboratory) circulating an Exalite 389 dye with a p-dioxane solvent that could be tuned to the 3914.4 Å bandhead. The process used to produce the desired pump laser wavelength from a Nd:YAG laser is very inefficient, and the energy level of the pump beam was marginal at best. This, coupled with the inefficiency of the detection optics, made detection of the induced fluorescence signal very difficult. While a very weak signal was consistently detected during the experiments, the pulse-to-pulse variations of the laser energy made the detected signal marginal and no conclusive demonstration was possible. A second attempt was made by using the frequency-tripled Nd:YAG beam to pump a Stilbene 420 dye with a methanol solvent to produce a beam at the 4278.1 Å bandhead of the (0,1) band of the N_2^+ first negative system. Again, after repeated experiments, it was found that a satisfactory demonstration could not be obtained using such a low-energy pump source with such high pulse-to-pulse variation.

A repeat of the experiment is planned. The electron beam and flow aspects of the experiment worked reliably and well. The LIF prospects are much improved, as we have recently obtained a Lambda Physik excimer-pumped dye laser system. This will allow strong pumping of the 3914.4 Å bandhead of the (0,0) N_2^+ system as originally planned.

2.2 Pulsed Electron-Beam Fluorescence

As mentioned above, PEBF is based on the ability of the pseudospark switch to generate high-current electron beams.[5,6] These beams have general characteristics as follows: electron energy 15 kV or higher; current of order 100–1000 kA; pulse length of order 10 ns; diameter around 1 mm. A schematic of an experiment employing PEBF as a diagnostic is given in fig. 2. The setup shown is identical to that normally seen in the use of EBF: the electron beam is passed through the flowfield and collected with a Faraday cup, while the fluorescence induced by inelastic electron-molecule collisions is collected and analyzed. Available information includes species density, temperature and velocity distribution function.[2,7,8]

Motivation for use of PEBF lies in the following:

- Significant ionization takes place in the beam path, leading to beam self-focusing and hence collimation even at quite high densities.
- The beam causes excitation which is collisionally quenched at high densities. This leads to a Stern-Vollmer-like form[1] for the emitted radiation integrated over one or more pulses, and the integrated signal loses its dependence on density as in EBF. However, the rapidity of onset of the beam current means that the peak intensity measured

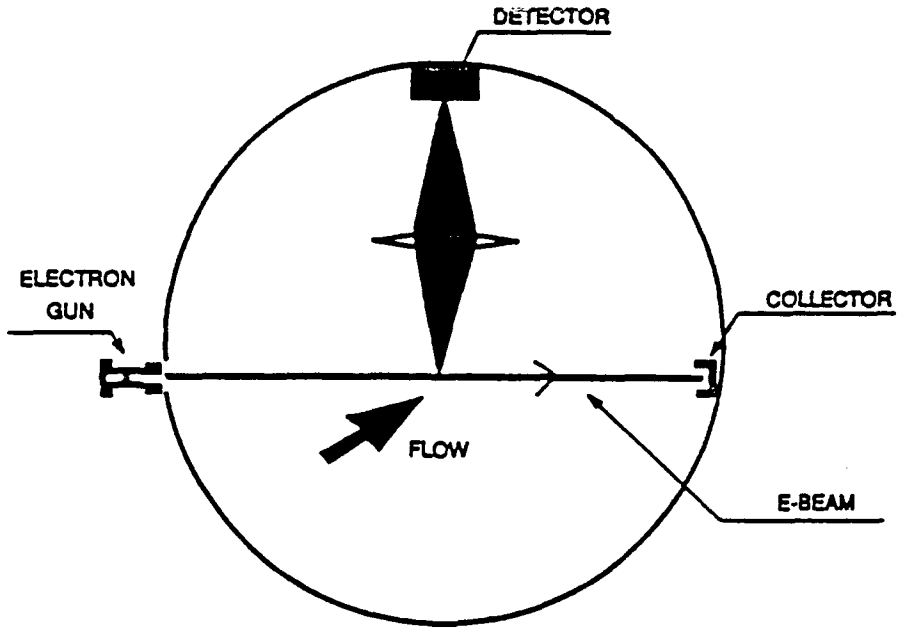

Figure 2: Schematic of pulsed electron-beam fluorescence experiment.

during a pulse retains full density dependence even when the signal is dominated by collisional quenching.

- The excitation is not species- or state-dependent. While this is a partial disadvantage compared to LIF in that individual states cannot be selectively probed, several advantages accrue:
  - Electron excitation acts on the majority components of the flow, so that there need not be an optically absorptive seed gas.
  - Radiation from different species contains different spectral lines, so that mixing flowfields may be instantaneously visualized without need of tuning a laser through several absorptions.
  - The optical signal is orders of magnitude stronger than in either LIF or EBF.

Fig. 3 shows a schematic of the pulsed electron gun, which takes the form of a high-voltage gas switch of pseudospark geometry.[5] The pseudospark chamber consists of two disc-shaped molybdenum electrodes which have on-axis holes approximately 3mm in diameter. These electrodes are kept at a constant separation of about 5mm. The electrodes are supported by cups in order to disallow any short-path surface breakdowns when the switch holds voltage. A tungsten wire in the cathode backspace provides the trigger electrode.

The gun is the discharge point of a high-power charging circuit, shown in fig. 4. A dc power supply charges a bank of doorknob capacitors through a 10MΩ air-cooled charging

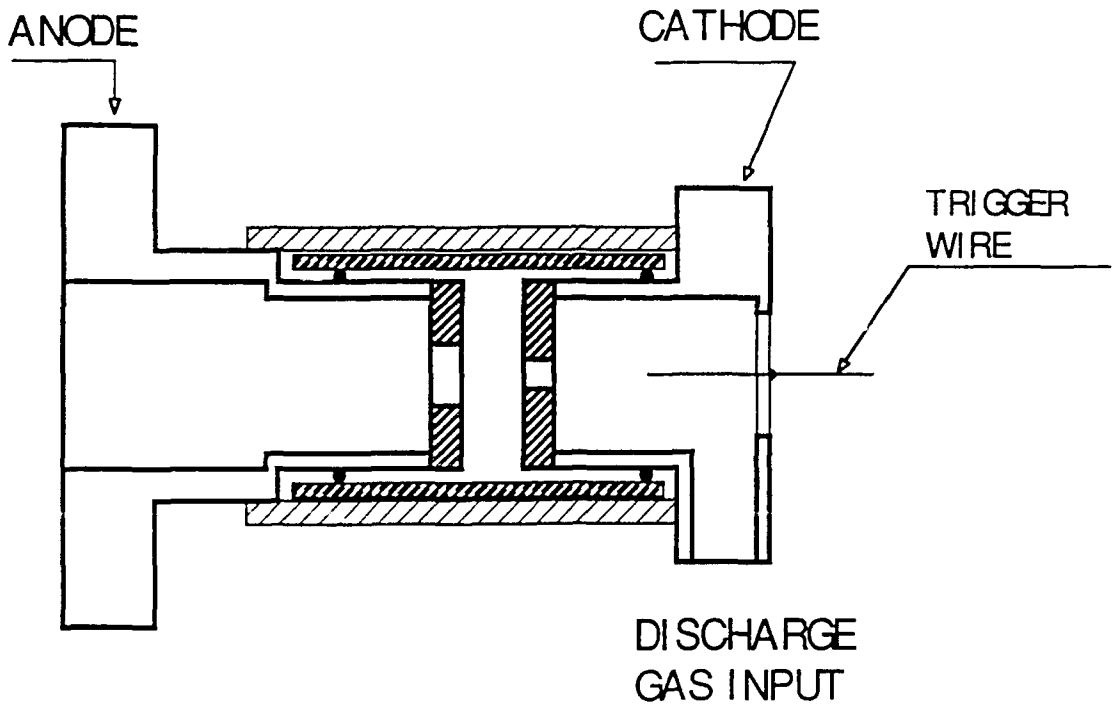

Figure 3: Pulsed electron gun schematic.

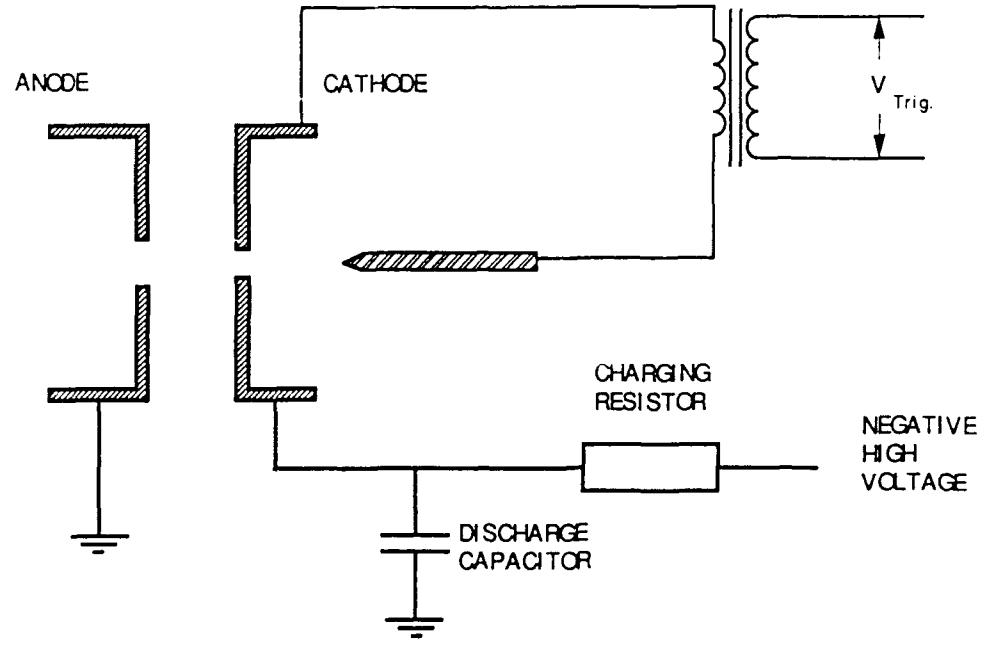

Figure 4: Charging circuit for electron gun.

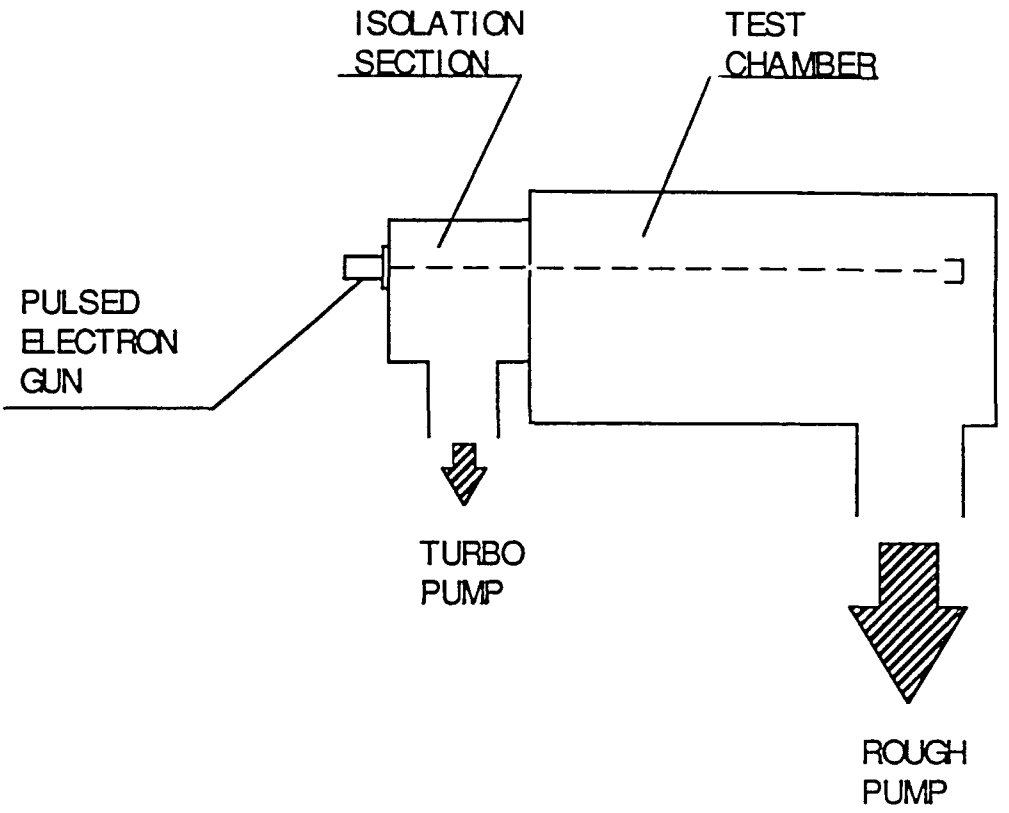

Figure 5: Vacuum and differential pumping setup.

resistor. The negative side of the charging network attaches to the cathode, while the anode is grounded.

With the pseudospark chamber maintained at less than 200 microns of helium, the apparatus is on the reverse side of the Paschen curve, so the breakdown strength is in excess of 30 kV. Breakdown is initiated by a positive pulse of about 2 kV (relative to cathode potential) applied to the trigger electrode. The trigger pulse is initiated by firing an SCR, which dumps 600 V from a small capacitor bank into the primary of the stepup pulse transformer shown

The switch discharges along the long path through the electrode holes. Electrons emitted from the rear face of the cathode cause a cascade discharge which passes through the central apertures. At the point of breakdown, runaway electrons at close to the breakdown energy are accelerated past the anode and continue ballistically into the flowfield test chamber, providing the diagnostic beam current. This process causes the switch to commute in a roughly 10-ns period, as the gas between the electrodes is brought to nearly full ionization. The capacitor energy is sunk into a 1Ω load resistor over a period of several hundred nanoseconds; during this period, the switch voltage drops to the cathode fall voltage ($\sim$ 100 V) and no further high-energy electrons are generated. However, a large current of low-energy ($\sim$200 V) electrons is generated during the main discharge period.

Extraction of electrons from the gun into the tank or test chamber, which is generally at higher pressure, requires differential pumping at the interface to take place. This is shown in fig. 5. In order to isolate the effect of tank pressure and gas composition from electron gun operation, a section is maintained at vacuum between the gun and the tank by a 9-inch

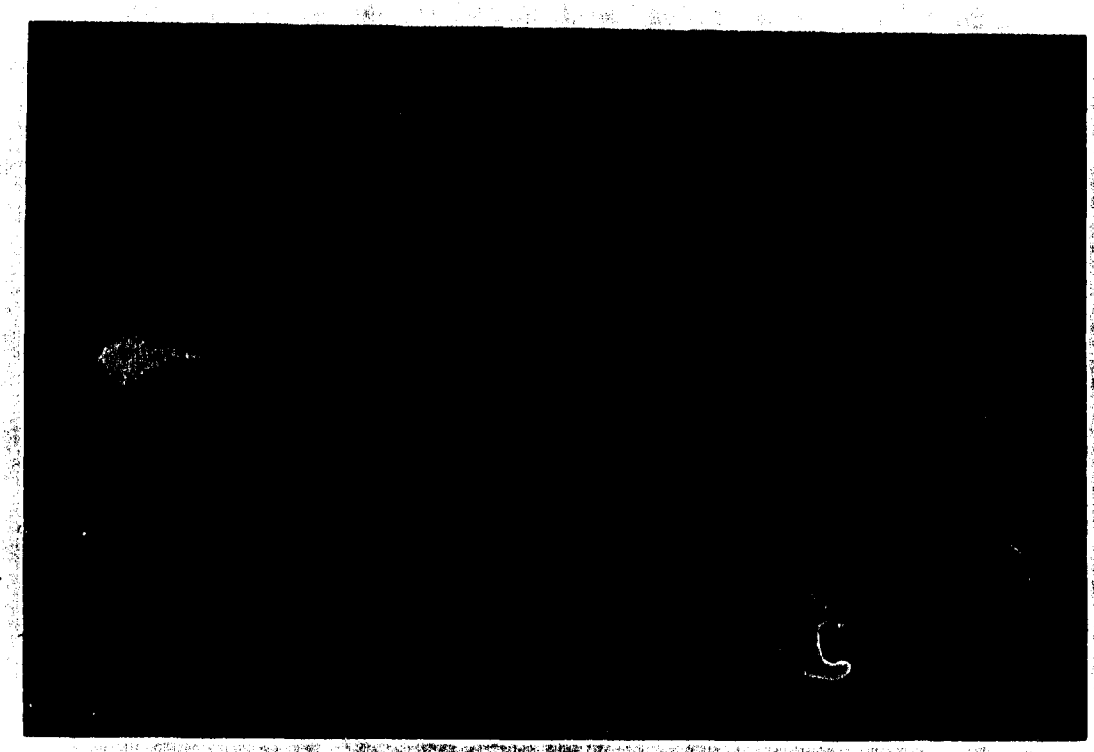

Figure 6: Beam fluorescence in static helium: a single pulse exposure. (Reproduction of photograph.)

turbopump. The beam passes through apertures variable from 0.5 to 2 mm. Leakage takes place through these from both the test chamber and the gun; a small fraction of the leaked gas crosses from the test chamber into the electron gun.

This gas contamination is the process which limits the chamber pressure at which the gun can operate. With the smallest apertures in place, the electron beam can be generated at test section pressures approaching one atmosphere.

Because of leakage into the vacuum isolation section, the helium supply must be continuously maintained. A gas manifold allows metered amounts of helium to be bled into the apparatus; the bleed rate together with the switch-side aperture determine the gas pressure at which the gun operates.

In order to investigate the properties of the pulsed e-beams, the electron gun is mounted on a two-meter vacuum tank.While it would be more realistic to verify diagnostic operation in an actual wind tunnel, the low duty ratio of the electron beam allows its use in the simpler setting of a static gas maintained in the tank.

A variety of ports are available for visual, photographic or photometric observation. A photomultiplier tube can be mated for quantitative analysis of the emitted radiation. Due to the great intensity of the fluorescence, no collection optics are necessary; indeed, an order or two of density filters are needed to avoid saturating the photocathode.

Fig. 6 shows a photograph of the fluorescence excited in static helium by the electron beam. The signal level is such that a single pulse is sufficient to expose the film, rendering

visualization along a line through the gas an easy matter. Color photographs taken in static gases of helium, argon and nitrogen show distinctly different hues, which should allow rapid mixing processes to be directly photographed.

The electron gun has demonstrated its ability to generate a reliable, triggered electron beam. At present our instrumentation capability does not allow instantaneous total beam current measurements, but based on peak switch current and on the amount of light generated, we believe the beam current to be 500 to 1000 amps peak. This is consistent with the observations of Benker *et al.*.[6]

The pulsed electron beam produced by the pseudospark switch appears to be a promising tool for flow diagnostics. The device is capable of reliably producing an electron beam of nanosecond duration with kiloamp-range peak current. Furthermore, the beam is well collimated and propagates without spreading over a wide range of pressures, and can be triggered on demand. However, good performance is contingent on precise control of electrode alignment and chamber pressure, and on elimination of all surface and gas impurities.

Preliminary data indicate that the device can be used as a point-density probe under conditions where standard continuous-beam electron fluorescence techniques fail due to collisional quenching. The upper limit for such density measurement is at present unknown, but is expected to be roughly 0.1–1 atmosphere.

In addition, the pulsed electron beam shows great promise as a device for direct flow visualization. The fact that the beam produces clearly visible and easily photographed fluorescence over a wide range of densities, along with the extremely short time scale involved, indicates that the device can be used as a sort of flashlamp to light up a flowfield in a way unmatched by existing techniques. It should be noted that the signal level is sufficient that the signal should be easily measurable even in high-temperature self-luminous flows. This holds promise for the study of, for example, thruster plumes.

Work is continuing towards the following practical diagnostic goals:

1. Demonstration of visualization of two-component mixing flows;
2. Determination of the upper bound of density that can be sensitively probed using PEBF;
3. Investigation of magnetic beam spreading/deflection techniques for two-dimensional visualization;
4. Application of PEBF to determination of species density profiles in electrothermal thruster plumes.

In addition, we are working on a compact, gas-triggered version of the switch for use in flight testing.

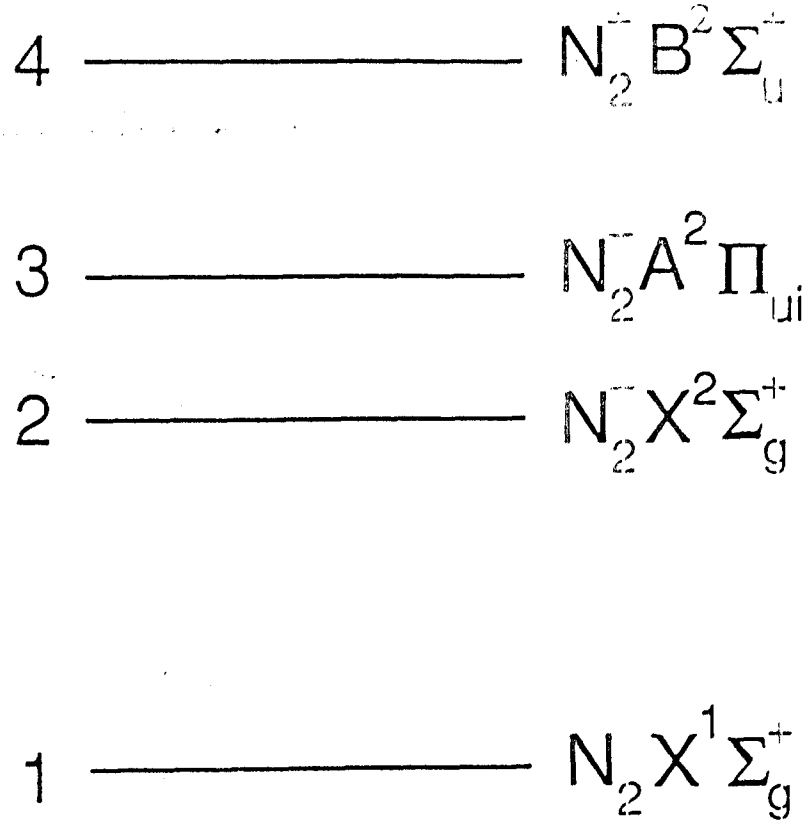

Figure 7: Energy levels of the N_2^+ first negative system considered in the rate-equation model.

3 Theoretical Understanding of Pulsed Beam Diagnostics

Our concern in this part of the work is the understanding of the production of radiation from a gas excited by a time-dependent electron beam. To this end, we have chosen the N_2^+ first negative system as a representative case of most general use.

An approximate solution of the time-dependent, zero-spatial-dimension equations for a constant beam turned on at $t = 0$ is given in ref. [3]. A more detailed solution of the several rate equations will now be briefly described.

We consider the four electronic energy levels of N_2 shown in fig. 7, the ground state of N_2 and the lowest three electronic levels of the ion N_2^+. The processes which connect the levels are electron impact ionization, photoionization, electron excitation, photoexcitation, and inverse processes (three-body and radiative recombination). Vibrational sublevels are considered individually. The cross sections for the processes considered are those used in ref. [1].

Fig. 8 presents a representative result of this model. The conditions assumed are the following: nitrogen gas initially in thermal equilibrium at 300 K, with density 10^{17} cm^{-3}, irradiated with a pulsed beam of 40-keV electrons, of current density 20 mA/cm^2, lasting 10 ns. Shown are the radiative intensities of the (0,0), (0,1), (1,0), (1,1), and (2,2) vibronic transitions of the N_2^+ first negative system following the pulsed beam (for times $t > 10$ ns).

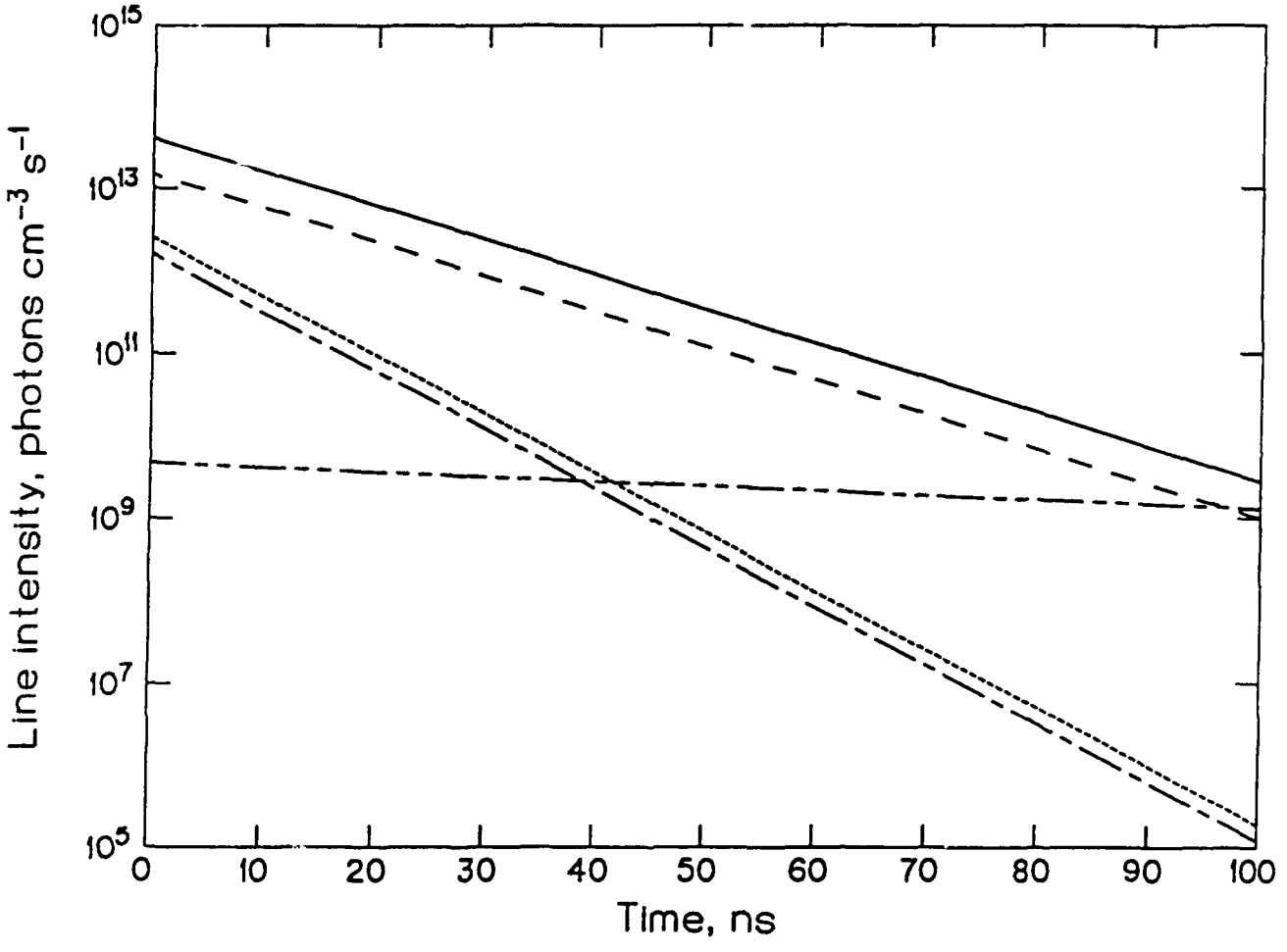

Figure 8: Radiative intensities from the (0,0), (0,1), (1,0), (1,1), and (2,2) vibronic transitions of the $N_2^+ B^2\Sigma_u^+ \rightarrow X^1\Sigma_g^+$ system folowing irradiation by a pulsed electron beam.

4 Conclusions

The electron-photon fluorescence technique still appears to be an attractive prospect for attaining quench-free diagnostics of intermediate-density supersonic and hypersonic flows. In addition, high-current pulsed electron beam diagnostics, a possibility unforeseen at the time of proposal, holds great promise for a simple, high-signal technique for visualization and point measurement in flows of near-atmospheric density. Further work on both these techniques is in process.

5 Publications resulting from the present support

The following publications were supported in full or in part by this contract:

1. S. H. Kang and J. A. Kunc, "Viscosity of high-temperature iodine," Phys. Rev. A., in press.

2. J. A. Kunc, "Vibration-translation exchange in diatom-diatom collisions," J. Phys. B, in press.

3. S. H. Kang and J. A. Kunc, "Molecular diameters in high-temperature gases," J. Phys. Chem., in press.

4. J. A. Kunc and W. H. Soon, "Electron Boltzmann equation in nonthermal plasmas," Phys. Rev. A **43**, 4409 (1991).

5. W. H. Soon and J. A. Kunc, "Kinetics and continuum emission of negative atomic ions in partially ionized plasmas," Phys. Rev. A **43**, 723 (1991).

6. R. M. Wojcik, J. H. Schilling and D. A. Erwin, "Rarefied flow diagnostics using pulsed high-current electron beams," AIAA-90-1515 (1990).

7. W. H. Soon and J. A. Kunc, "Radiation of partially ionized atomic hydrogen," Phys. Fluids B **2**, 2833 (1990).

8. J. A. Kunc, "Central-force potentials for interaction of rotationally and vibrationally excited molecules," J. Phys. B **23**, 2553 (1990).

9. W. H. Soon and J. A. Kunc, "Thermal nonequilibrium of partially ionized atomic oxygen," Phys. Rev. A **41**, 825 (1990).

10. J. A. Kunc and W. H. Soon, "Collisional-radiative nonequilibrium in partially ionized atomic nitrogen," Phys. Rev. A **40**, 5822 (1989).

References

[1]E. P. Muntz, AGARDograph 132, 1968.

[2]K. A. Buetefisch and D. Vennemann, Prog. Aerosp. Sci. **15**, 217 (1974).

[3]E. P. Muntz, J. A. Kunc, and D. A. Erwin, AIAA Thermophysics Conference, Honolulu, 1987.

[4]W. Benker, J. Christiansen, K. Frank, H. Gundel W. Hartmann, T. Redel, and M. Stetter, IEEE Trans. Plasma Sci. **17**, 754 (1989).

[5]K. Frank and J. Christiansen, IEEE Trans. Plasma Sci. **17**, 748 (1989).

[6]W. Benker, J. Christiansen, K. Frank, H. Gundel, W. Hartmann, T. Redel, and M. Stetter, IEEE Trans. Plasma Sci. **17**, 754 (1989).

[7]L. N. Harnett and E. P. Muntz, Phys. Fluids **15**, 565 (1972).

[8]T. Holtz and E. P. Muntz, Phys. Fluids **26**, 2425 (1983).